CRYSTAL GROWTH & DESIGN

pubs.acs.org/crystal

Article

Structural Characterization of Pyrrolidine–Including Structure II Clathrate Hydrates

Sanehiro Muromachi,* Hassan Sharifi, Saman Alavi, John A. Ripmeester, and Peter Englezos

Cite This: *Cryst. Growth Des.* 2021, 21, 2828–2836

Read Online

ACCESS | Metrics & More | Article Recommendations | Supporting Information

ABSTRACT: Clathrate hydrates are host–guest crystalline compounds which can capture both small gases such as H_2, CH_4, and CO_2 and larger guest molecules which are in the liquid state. Large guests (LGs) such as tetrahydrofuran (THF) can strongly stabilize the structure II clathrate hydrate under moderate conditions and provide a substantial number of small cages for the encapsulation of smaller guest gases. Most hydrocarbon LGs are volatile and immiscible in water, and even the water-miscible LGs such as THF are still volatile. The use of these LGs requires a recovery process in applications based on hydrates. Amines are one chemical group of alternative LGs which have low vapor pressure compared to hydrocarbon LGs. In this study, we report structural characterization for clathrate hydrates formed with the cyclic amine pyrrolidine (PL) and the structurally related THF. Crystal samples were formed from aqueous solutions of PL and THF with several ratios. Lattice constants determined by the single-crystal X-ray diffraction increased with the increase of PL content in the hydrate. Inspection of the cage size found that $5^{12}6^4$ cages expand due to PL inclusion, while the empty 5^{12} cages do not expand to the same degree. The refined X-ray diffraction structure suggests that the PL is incorporated in the large cage without forming hydrogen bonds with the cage water molecules. Molecular dynamics simulations also support weak hydrogen bond interactions between PL and water molecules.

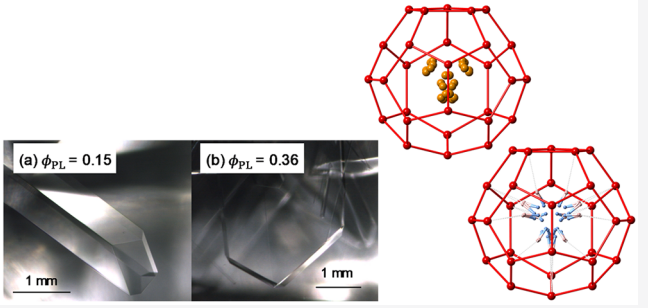

1. INTRODUCTION

Clathrate hydrates are host–guest compounds formed by the cooperation of water (host) and small molecules (guest), such as hydrocarbons or inert gases in which water molecules form space filling hydrogen bonded cages which encapsulate the guests.[1−3] Clathrate hydrates with gas phase guests usually form under high pressure and low temperature conditions and incorporate small gas molecules. Inclusion of large guests can usually moderate formation pressure and temperature conditions and form simple hydrates or binary hydrates with smaller gas molecules. There are three basic structures for clathrate hydrates, i.e., structure I (sI), structure II (sII), and structure H (sH), that form with suitably sized guest molecules.[1−3] Each structure is composed of a combination of different types of cages, e.g., a dodecahedron (5^{12}) which consists of 12 pentagonal faces, a tetrakaidecahedron ($5^{12}6^2$) which consists of 12 pentagonal faces and two hexagonal faces, and a hexakaidecahedron ($5^{12}6^4$) which consists of 12 pentagonal faces and four hexagonal faces. Different gas capacities and selectivities result from a combination of the cages and the size and chemical nature of the guests. The sI hydrate forms from small gas phase guest molecules like CH_4 and CO_2 and smaller guests like H_2, O_2, N_2, and Ar form sII hydrates. The sII and sH hydrates can incorporate larger guest (LG) molecules, e.g., cyclopentane and methylcyclohexane, respectively. The sII phases often encapsulate additional smaller guests into the 5^{12} cages of the phase, while the sH phases require smaller guests in the 5^{12} and $4^35^66^3$ cages. Since sII hydrates in the presence of LG form under more moderate pressure and temperature conditions compared to the sI hydrates, e.g., 1 MPa at 286 K with sII THF + CO_2 hydrates,[4,5] compared to >4 MPa at 286 K for sI CO_2 hydrate, they are potential media for transportation of natural gases,[6,7] desalination[8,9] and CO_2 capture.[9,10] However, LGs of sII hydrates are often volatile, flammable, and toxic.

Utilization of low-quality or abundant and cleaner energy in the short term can be a key factor in sustainable development.[11−15] Clathrate hydrates can capture a variety of gases such as H_2, CO_2, N_2, and CH_4.[16−18] In some gas mixtures containing CO_2, the concentration of CO_2 in the hydrate phase is enriched compared to that in the original gas phase, and so clathrate hydrate formation can be utilized for CO_2 separation and capture.[19−26] The CO_2 capture process with LG requires additional facilities such as a condenser and liquid–liquid

Received: December 30, 2020
Revised: April 18, 2021
Published: April 26, 2021

https://doi.org/10.1021/acs.cgd.0c01745
Cryst. Growth Des. 2021, 21, 2828–2836

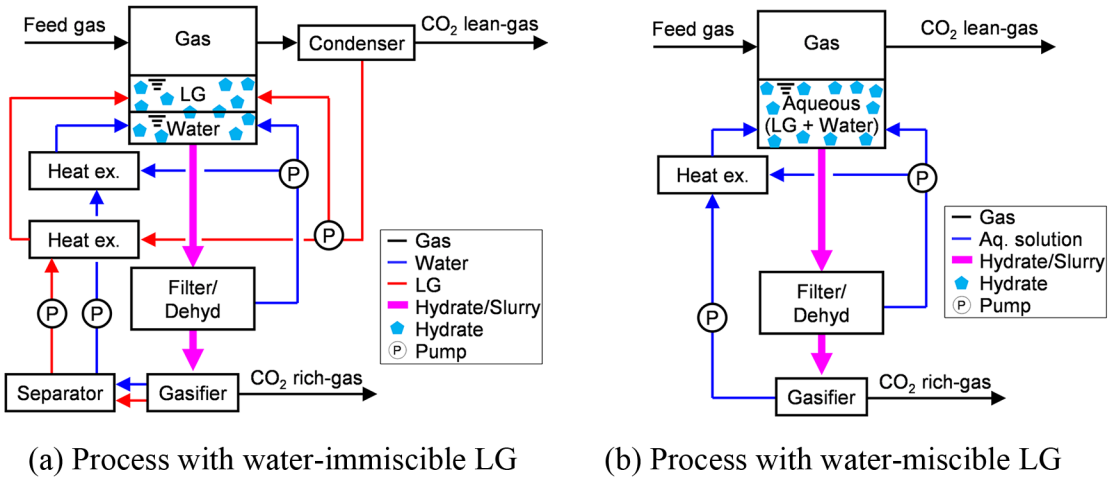

(a) Process with water-immiscible LG (b) Process with water-miscible LG

Figure 1. Conceptual process diagram of the CO_2 gas separation process based on clathrate hydrates for water-immiscible and water-miscible LGs.

separator for the hydrate formation and separation process. Figure 1(a) illustrates a CO_2 gas separation process based on water-immiscible large cage guests such as alkanes. When alkanes are used for the process as large guests for sII hydrates, their high volatility necessitates the introduction of an additional process for condensation of the large guest from the refined gas stream. Furthermore, since many of the LG are immiscible with water, mixing and separation processes of the two liquid water and LG phases are also necessary to promote rapid hydrate formation and to avoid accidentally plugging of the facilities. Figure 1(b) shows a process with a water-miscible LG. When a water-miscible LG is used in the process, the clathrate hydrates form from a single liquid phase, i.e., an aqueous solution of the LG. This makes it possible to simplify the process, and in these cases, only one cooling loop is necessary for the aqueous phase. Ethers, such as THF, tetrahydropyran,[27,28] and *tert*-butyl methyl ether, are water-miscible (or partially water-soluble) LGs for sII and sH hydrates, respectively.[2,29] While these water-miscible LGs are useful for simplifying the gas separation process, they still have considerable vapor pressures, i.e., 23 kPa at 300 K for THF.[30] If vapor pressure of the LGs can be suppressed, even to a limited degree, the process can be made both simpler and safer and has lower energy requirements.

Amines are widely used for CO_2 capture as an absorbent,[31] and they are also LGs for sII and sH hydrates.[32−38] Due to the lower volatility and vapor pressure of amines compared to that of ethers, the uses of these former LGs in hydrate formation can be simplified. Pyrrolidine (PL) is a cyclic amine with a vapor pressure of 6.5 kPa at 298 K, which has a similar molecular size and structure (and is isoelectronic) to the cyclic ether and alkane THF and cyclopentane. The choice of PL primarily demonstrates that alternatives to THF with lower vapor pressure can be possible for sII hydrate formation. In particular, THF has a vapor pressure of 23 kPa at 300 K, while that of PL is about 6.5 kPa at the same temperature. As we described above, the process design is a step-by-step investigation for further improvement on gas capture and storage by sII hydrates.

Below the freezing point of water, PL forms a stoichiometric hexahydrate, not a clathrate;[36,39] however, above the freezing point of water and under the pressure of a secondary guest gas pressure, this amine forms sII clathrate hydrates.[32,36] This is an advantage for use in gas separation processes based on clathrate hydrate formation at near ambient temperatures because it enables extra cooling of the aqueous phase to facilitate hydrate formation without plugging the flow by ice which can occur during the formation of simple clathrate hydrates from the LG alone. Although the molecular structure of PL is quite similar to THF, it is reported that PL cannot form clathrate hydrates either by itself[1] or with CO_2.[32] This is probably due to the relatively larger molecular size of PL (compared to THF) which can be barely incorporated in the $5^{12}6^4$ cage and the strong chemical interaction between CO_2 and PL in the aqueous phase which disrupts the hydrogen bonding network of water molecules around them. Such complicated interactions may lead to modification of the structure of clathrate hydrate.[40−42]

In this work, we studied amine hydrates formed with the assistance of relatively limited amounts of THF and analyzed the effects of the amine on the sII hydrate structure which is suitable for gas capture and storage. We characterized the hydrates formed with PL and THF by melting temperature measurements, X-ray diffraction analyses, and solution-state NMR measurements. Molecular dynamics simulation was also used for investigating the mutual interaction between host and guest molecules in this sII double hydrate. The results suggest modification of the hydrate formation process by introducing water-miscible and low volatile LGs for improving hydrate-based gas capture technologies.

2. EXPERIMENTAL SECTION

2.1. Materials. We used water filtered by activated carbon and sterilized with an ultraviolet lamp. The electrical resistivity of the water was >18.2 MΩ. For melting temperature measurements and gas separation performance tests, PL (Sigma-Aldrich, >99%) and THF (Alfa Aesar, >99%) were used without further purification. For X-ray diffraction analyses, PL (Sigma-Aldrich, >99%) and THF (Sigma-Aldrich, >99.9%) were used without further purification. For NMR measurements, we used deuterium oxide (Wako Pure Chemical Industries, >99.9%) as a solvent to simplify the interpretation of the guest spectra.

2.2. Characterization of the Clathrate Hydrates. For the melting temperature measurements for the PL + THF hydrates, four aqueous solutions were used in the experiments. We prepared the sample solutions in glass vials with the aid of an electronic balance (Ohaus, Adventurer Pro AV313), and molar compositions in the solutions (x) were determined based on mass. We note that air

https://doi.org/10.1021/acs.cgd.0c01745
Cryst. Growth Des. 2021, 21, 2828−2836

remained in the glass vials and was not removed prior to experiments. Because the stoichiometric composition of the LG in the sII hydrates is 0.056, we used the fixed composition of total LG in the solutions ($x_{THF} + x_{PL}$) relative to water to be this value. The molar ratio of PL to total LG (THF + PL), $\Phi = x_{PL}/(x_{THF} + x_{PL})$, for the solutions was determined to be 0.078, 0.287, 0.505, and 0.933.

The measurements were performed in a water bath in which temperature was maintained by circulating cooling water. The glass vials filled with solution were initially frozen in a refrigerator at ~250 K and then placed in the water bath. A stepwise temperature increase with 0.5 K increments weas used to find the maximum temperature at which hydrates were present in the solutions. We determined this temperature to be the melting temperature of the hydrate. The system temperature was measured by a glass thermometer (Ever-safe, N16B) which was calibrated by a solid−liquid equilibrium temperature of water under ambient pressure. The measurement uncertainties were 0.5 K for the temperature and 0.002 for x.

Single crystals of the hydrate were also grown in a temperature-controlled water bath. Four sample solutions with Φ = 0, 0.105, 0.306, and 0.502 were prepared in glass tubes. Subcooling temperatures for crystal growth were 2−3 K. We observed crystals under a microscope (Edmund Optics, VZM-200i) and a CCD camera (Sentech, MC-152USB). After the hydrate crystals grew, the residual aqueous solutions were removed from the tube. The single crystal suitable for X-ray diffraction was selected and mounted on a CCD detector type diffractometer (Bruker AXS, SMART APEX). The crystal structures were solved and refined with SHELX.[43] The details of single-crystal X-ray diffraction analyses are provided in Tables S1 and S2 in the Supporting Information. Hydrogen atoms were manually placed on the LG molecules. Since THF and PL in $5^{12}6^4$ cages have numerous positions generated by symmetry operations, giving anisotropic displacement parameters for THF and PL is not physically reasonable. Thus, these parameters are left isotropic during the present refinement processes. The CIF crystallographic data of the hydrates formed with Φ = 0.502 are deposited in the Cambridge Crystallographic Data Centre (CCDC) under number 2045524.

Solution-state NMR measurements were also performed on the melted crystal solutions. The melted solutions were diluted with deuterium oxide and mounted on the NMR spectrometer (Bruker, Avance 500). From the peak areas of the hydrogen in CH_2 neighboring nitrogen in PL and oxygen in THF, the fraction of PL and THF in hydrate phase was determined. All the spectra recorded in this study are provided in Figure S1 in the Supporting Information.

2.3. Molecular Dynamics Simulations. Molecular dynamics simulations were performed by using DL_POLY program version 2.20 developed by Smith, Forester, and Todorov.[44] In the simulations, a 2 × 2 × 2 unit cell replica of sII hydrates of THF and PL was used. The disordered water proton positions in the sII hydrate unit cell were taken from Takeuchi et al.[45] The TIP4P/2005 model was used for intermolecular interactions of water molecules.[46] The General Amber Force Field (GAFF) was employed for THF and PL molecules to determine the Lennard-Jones parameters for the van der Waals interactions,[47,48] and the TraPPE model was used for methane.[49] The CHELPG method was used to determine nucleus-centered point charges on the guest atoms for the electrostatic interactions.[50] Structures of the two guest molecules were calculated at the B3LYP/aug-cc-pvdz level of theory using the Gaussian 09 suite of programs.[51] The PL molecule can be in two conformers with the amine hydrogen in the equatorial or axial position with respect to the five-atom heterocyclic ring. In agreement with previous quantum chemical studies,[52−56] the equatorial conformer was used as the most stable form of the guest. All the cross interaction Lennard-Jones parameters between atoms on different molecules were calculated by the Lorentz−Berthelot combining rules. The Ewald method was used to evaluate the electrostatic interactions with a relative error of 10^{-6} and an overall cutoff of 15 Å.[57,58] The guest molecules were kept rigid during simulations. The force field parameters are given in Table S3 of the Supporting Information.

The temperature and pressure of the simulation were maintained constant using a Nosé−Hoover thermostat-barostat[57,58] with relaxation times of 0.2 and 0.5 ps, respectively. The equations of motion were integrated at each time step of 1 fs. The system was equilibrated at the target temperature for 100 ps in the simulation followed by 1 ns of data gathering after equilibration. Periodic boundary conditions (PBCs) were used in three directions. The simulations were performed at 250, 260, and 270 K to observe the temperature effects on the hydrate phase properties.

3. RESULTS AND DISCUSSION

3.1. Characterization of the Clathrate Hydrates. The melting temperatures of the PL + THF hydrates formed from solutions with Φ = 0.078, 0.287, 0.505, and 0.933 are shown in Figure 2. The details of the melting temperature measurements

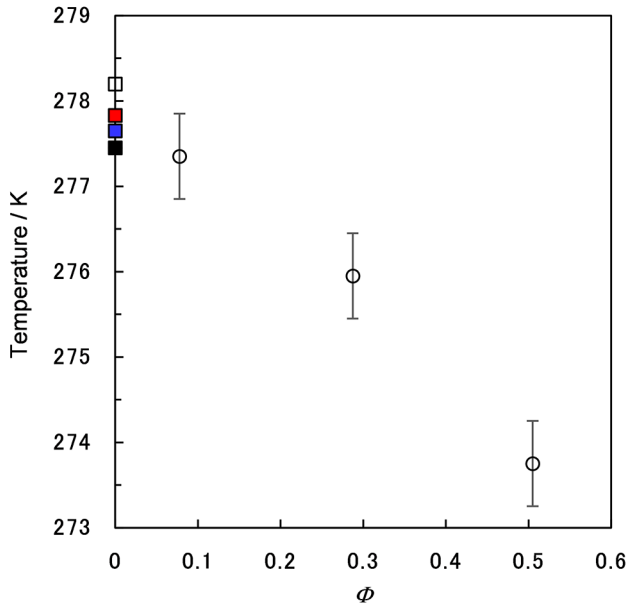

Figure 2. Melting temperature of the THF + PL hydrates as a function of the mole fraction of PL in the LG mixture. The total mole fraction of the LG mixture (THF + PL) in the aqueous solutions was ~0.056: ○, this work; □ (white), pure THF hydrate;[60] □ (red), pure THF hydrate;[62] □ (blue), pure THF hydrate;[59] and □ (black), pure THF hydrate.[61]

Table 1. Results of Melting Temperature Measurements for THF + Pyrrolidine Hydrates at Ambient Pressure

Φ	x_{PL}	x_{THF}	Melting temperature /K
0.078	0.0042	0.0502	277.4
0.287	0.0156	0.0386	276.0
0.505	0.0276	0.0270	273.8
0.933	0.0501	0.0036	>261.4

are provided in Table 1. The melting temperature with Φ = 0.078 was almost the same as that of the pure THF hydrate reported in the literature,[59−62] and the small mole fraction of PL only changed the melting temperature by a small amount. The THF + PL hydrates formed with Φ = 0.287 and 0.505 melted above the freezing point of ice and so can be formed under conditions of lower vapor pressure than pure THF hydrate. With Φ = 0.933, a stable solid was obtained below 262 K; however, this sample melted below 268.9 K. While the hexahydrate of pyrrolidine (not a clathrate) can form at 269.2

https://doi.org/10.1021/acs.cgd.0c01745
Cryst. Growth Des. 2021, 21, 2828−2836

K,[36] the solid phase at Φ = 0.933 melted below this temperature. Accordingly, the presence of THF may affect stability of the hexahydrate of pyrrolidine. These results verified that a secondary large guest is necessary to form a stable binary hydrate with a large content of PL above 273 K.

Single crystals formed under atmospheric pressure in the systems of THF + PL + water are seen in Figure 3. With Φ = 0.306, in Figure 3(a), highly symmetric crystals were observed, while with Φ = 0.502 in Figure 3(b), elongated crystals in which certain crystal faces grew are observed.

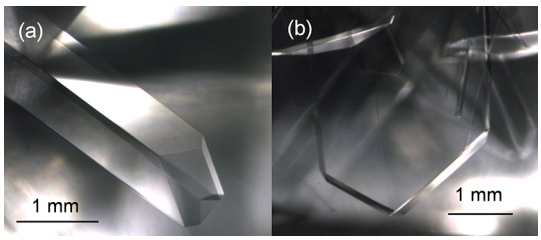

Figure 3. Pictures of the single crystals formed in the THF + PL + water systems: (a) Φ = 0.306 formed at 273.6 K and (b) Φ = 0.502 formed at 271.6 K.

The melted single crystals were subjected to solution ^{1}H NMR measurements which can give information for the ratio of PL to THF in the hydrate crystals (ϕ_{PL}). The obtained spectra are provided in the Supporting Information. Figure 4

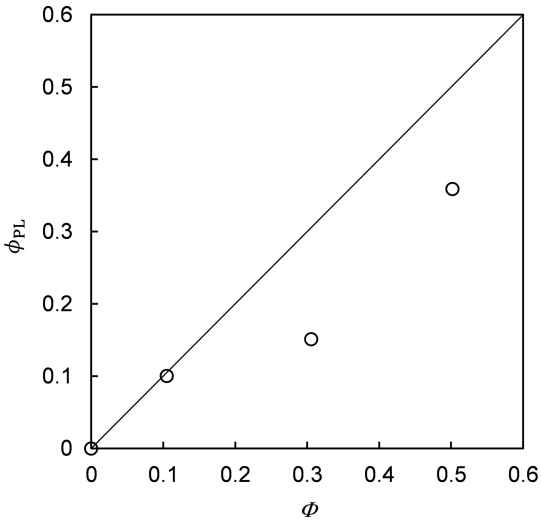

Figure 4. Fractionation of PL and THF between the solution phase and sII hydrate phase determined by solution-state NMR measurements. The line indicates the proportional relationship between ϕ_{PL} and Φ.

shows the relationship between ϕ_{PL} and Φ. The results showed that the single crystals formed with Φ = 0.105 contained PL in the hydrate phase in similar proportion as that in the aqueous phase. At higher Φ, THF was slightly enriched in the hydrate phase relative to the solution from which the hydrate was formed. In the THF−PL hydrate synthesis, the pyrrolidine changes the activity of the water, so it acts as an inhibitor which changes the melting point; but it is also a guest but not a good enough guest to stabilize the hydrate lattice by itself. Hence pyrrolidine must be "introduced" by a known hydrate forming guest, THF. This kind of inclusion was termed an "Einschleppung".[63]

The single crystals were subjected to the X-ray diffraction analysis at 173 K. All the tested crystals were determined to be the cubic structure II hydrate. The detailed information on the structural analyses is summarized in the Supporting Information, and the structural data with ϕ_{PL} = 0.36 (Φ = 0.502) were deposited in the structural database. Figure 5 shows the lattice

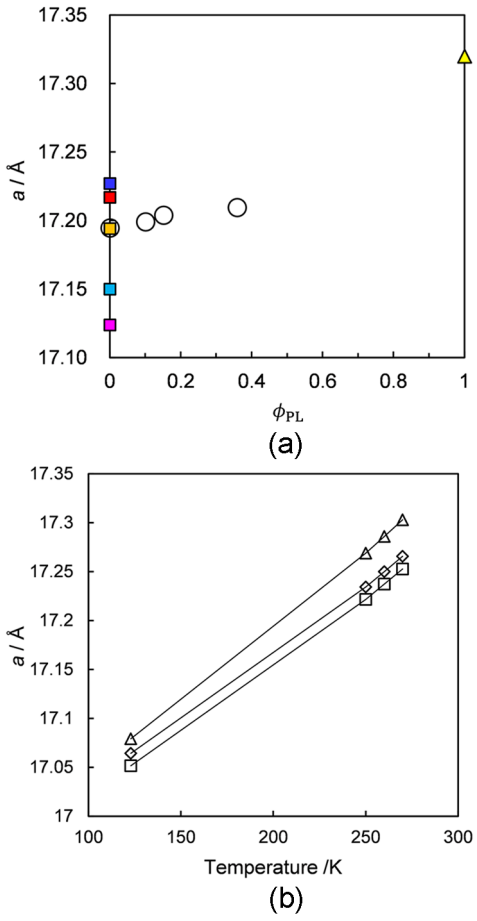

Figure 5. Lattice constants of THF + PL hydrates. (a) Lattice constants determined by single-crystal X-ray diffraction: ○ (white), this work at 173 K; □ (magenta), THF hydrate at 100 K;[64] □ (sky blue), THF hydrate at 125 K;[42] □ (blue), THF hydrate at 173 K;[65] □ (orange), THF hydrate at 173 K;[66] □ (blue), THF hydrate at 220 K;[36] △ (yellow), PL + CH_4 hydrate at 123.15 K.[32] (b) The temperature dependence of the lattice constants calculated by MD simulations: the hypothetical PL sII hydrate (△), the THF sII hydrate (□), and the PL + CH_4 sII clathrate hydrate (◊) with all small cages filled with methane.

constants (a) of the present hydrates at 173 K. This figure confirmed that our present data for pure THF hydrate (ϕ_{PL} = 0) are consistent with the literature data.[32,36,42,64−66] An increase of ϕ_{PL} slightly expands the lattice from pure THF hydrate (ϕ_{PL} = 0). With ϕ_{PL} = 0.36 (Φ = 0.502), the lattice constant is increased from that with ϕ_{PL} = 0.15 (Φ = 0.306). The present data were compared with those in reference 32 where a lattice constant of 17.320 Å at 123.15 K was given for PL + CH_4 hydrates formed from an aqueous solution with a 0.0556 mole fraction of PL. These data clearly show that the inclusion of methane in the structure strongly expands the

https://doi.org/10.1021/acs.cgd.0c01745
Cryst. Growth Des. 2021, 21, 2828−2836

lattice exceeding the increasing tendency depending on ϕ_{PL} for the hydrates formed with just THF and PL.

Average distances from cage centers to water oxygens ($\bar{d}$) in 5^{12} ($\bar{d}_S$) and $5^{12}6^4$ ($\bar{d}_L$) cages are shown in Figure 6(a). As well

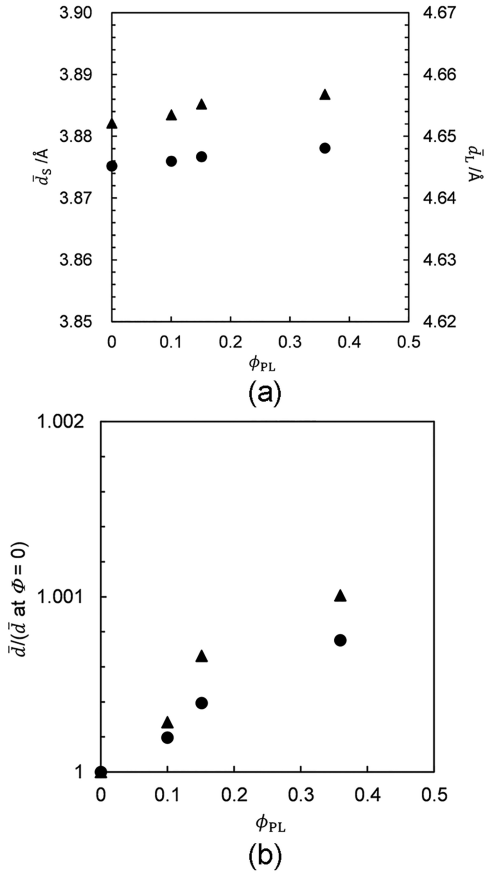

Figure 6. Average distances between water oxygen and cage center ($\bar{d}$): (a) $\bar{d}_S$ and $\bar{d}_L$ and (b) $\bar{d}/(\bar{d}$ at $\Phi = 0$) (pure THF hydrate). Symbols: ●, $\bar{d}_S$; ▲, $\bar{d}_L$.

as lattice constants, $\bar{d}_S$ increased due to an increase of Φ in both 5^{12} and $5^{12}6^4$ cages. Figure 6(b) shows the ratio of $\bar{d}/(\bar{d}$ at $\Phi = 0$) (pure THF hydrate). At ϕ_{PL} = 0.15 and 0.36 (Φ = 0.306 and 0.502, respectively), the cages expand anisotropically, that is, the $\bar{d}_L$ cage increased slightly more than in the 5^{12} cage. Therefore, it was suggested that the $5^{12}6^4$ cages expanded due to PL inclusion and that empty 5^{12} cages do not uniformly follow the $5^{12}6^4$ cage expansion. Because of PL inclusion, the $5^{12}6^4$ cage requires nonuniform expansion which may lead to an unstable sII hydrate structure. Formation of pure PL hydrate with many empty 5^{12} cages is difficult, while formation of hexahydrate without empty voids is possible in the pyrrolidine−water system.[36] The expanded structure at a higher PL content may be stabilized by filling 5^{12} cages with small guests,[32] as was also observed in cases such as carbon tetrachloride sII hydrate.[1]

The single-crystal structure refinement on the sample with ϕ_{PL} = 0.36 (Φ = 0.502) was also performed. The present crystal structure analysis showed that both THF and PL were incorporated in the $5^{12}6^4$ cage of the structure II hydrate. Figure 7 shows the distribution of THF and PL molecules in the $5^{12}6^4$ cage. Although these two guest molecules are similarly shaped, the additional hydrogen atom attached to the

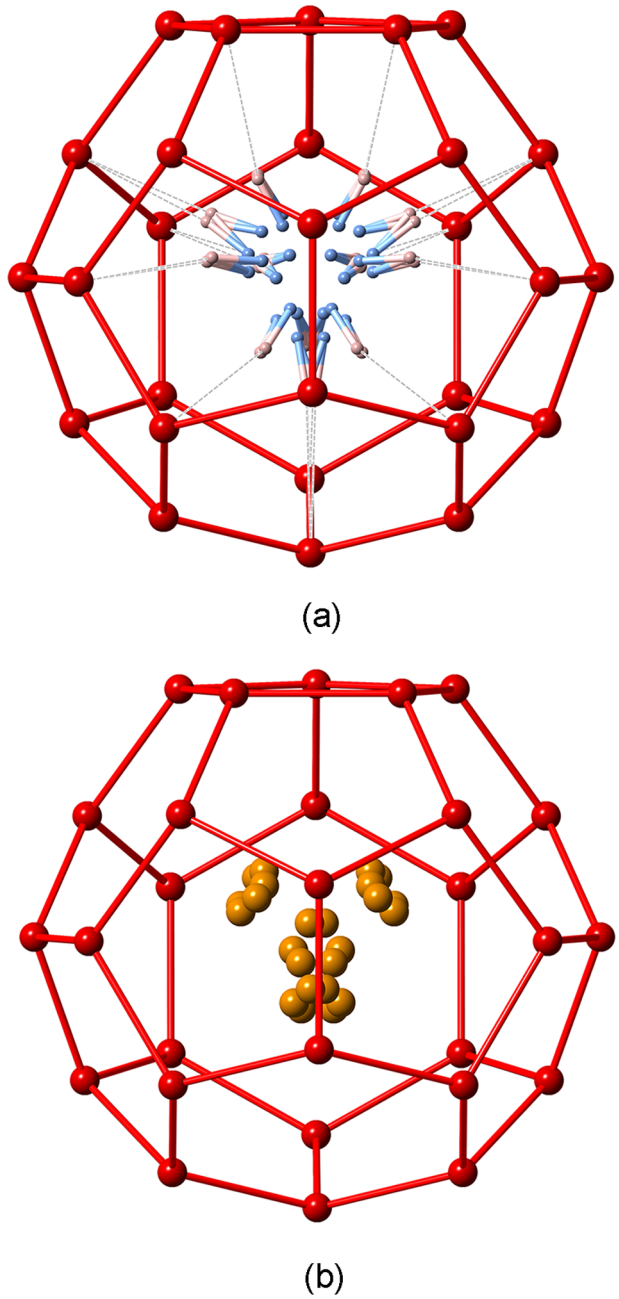

Figure 7. Distribution of (a) THF and (b) PL molecules in the $5^{12}6^4$ cage revealed by structure refinement. Hydrogen atoms in water and the hydrocarbon chain are omitted for clarity: red, oxygen atom in water; orange, oxygen atom in THF; pale pink, hydrogen atom in PL; blue, nitrogen atom in PL; solid line, hydrogen bonding between water molecules; dashed line, the nearest position of the hydrogen atom in the amino group to the cage water. Possible positions of atoms duplicated by symmetry operations are shown.

nitrogen atom in PL exceeds the size limit for the large cage. The distance between the oxygen atoms of the nearest cage water and the hydrogen and nitrogen atoms of the amino group in PL were ∼2.7 and 3.6 Å, respectively. Since hydrogen bond lengths between water molecules (H−O distance) found in the present structure were ∼1.9 Å, it is not clear that there was hydrogen bonding between PL and the cage water in this structure. The oxygen atom in THF is aligned toward the hexagonal face of the $5^{12}6^4$ cage. The distance between the cage water and oxygen atom in THF was ∼3.5 Å which is

https://doi.org/10.1021/acs.cgd.0c01745
Cryst. Growth Des. 2021, 21, 2828−2836

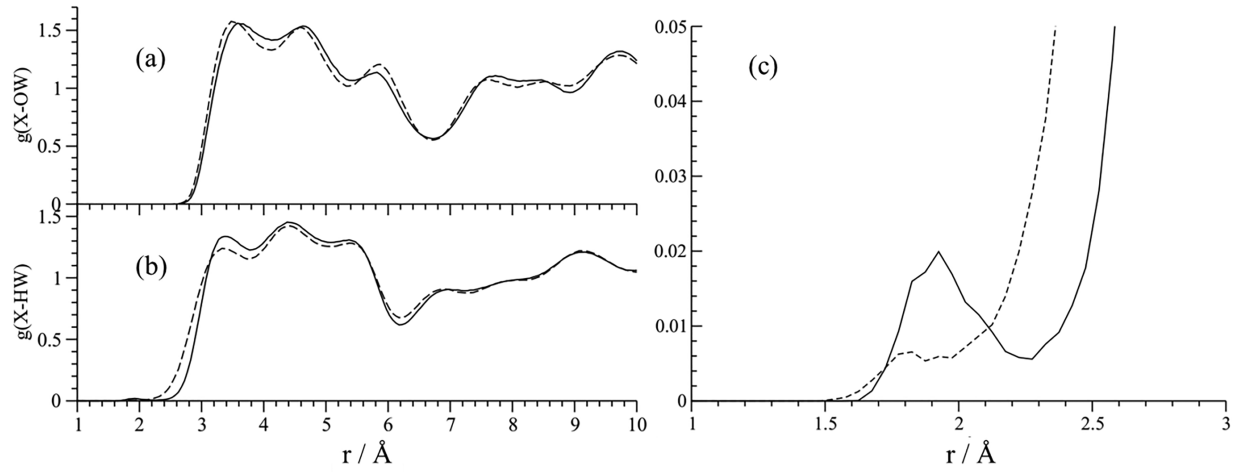

Figure 8. (a) The radial distribution function (g) of the THF oxygen (OS) and water oxygen (OW). The full line represents PL, and the dashed line represents THF. (b) The RDF for the THF oxygen (OS) and water hydrogen (HW). (c) A zoomed in view of the RDF for the THF oxygen (OS) and water hydrogen (HW) in the range of 1−3 Å. The peaks in between 1.8 and 1.9 Å represent the proton accepting hydrogen bonding of the large cage guests with the sII large cage water molecules.

longer than the H−O distance of PL and water. Cage occupancies of the THF and PL in the $5^{12}6^4$ cage were determined to be 0.55 and 0.42, respectively. These values are not exactly the same as for ϕ_{PL} = 0.36 which was found by solution-state NMR measurements, but they agreed with each other considering measurement uncertainties.

3.2. MD Simulations. The calculated lattice constants for the hypothetical sII PL hydrate, the sII THF hydrate, and the PL + CH_4 hydrate with all small cages occupied by methane molecules are given in Figure 5(b) for temperatures from 123 to 270 K. The lattice constants for the PL hydrate are larger than those of THF. Addition of CH_4 into the hydrate small cages has the effect of increasing the predicted lattice constants of the unit sII cell. At 123 K, the magnitudes of the differences between the MD lattice constant for THF and that of the sII PL + CH_4 hydrate are smaller than those measured experimentally.

The radial distribution functions (RDFs) which indicate hydrogen bonding among THF, PL, and water molecules in the large cages of the sII hydrate are shown in Figure 8 where g and r denote RDF and radial distances between atoms, respectively. In Figure 8(b), the radial distribution function of the THF oxygen (OS) and the water hydrogen (HW) is shown. The radial distance between 1 and 3 Å of this RDF is shown in Figure 8(c) which is the region of hydrogen bonding. The RDF peaks of the two guests between 1.8 and 1.9 Å show weak hydrogen bonding between the guests and cage water where water is the proton donating group in the hydrogen bond. Although both hydrogen bonds are weak, the PL shows a greater degree of hydrogen bonding than THF.

The configurational energies (total kinetic energy) for the hypothetical sII PL hydrate, the sII THF hydrate, and the PL + CH_4 hydrate with all small cages occupied by methane molecules are given in Figure 9 for temperatures from 123 to 270 K. The configurational energies of the PL and THF hydrates are very similar in magnitude, but the CH_4 molecules significantly lower the configurational energy of the unit cell, stabilizing the hydrate phase.

Since the configurational energies in the hydrate phase are almost the same for PL and THF, differing from the results of some previous work on other cyclic amines,[33,37] other chemical

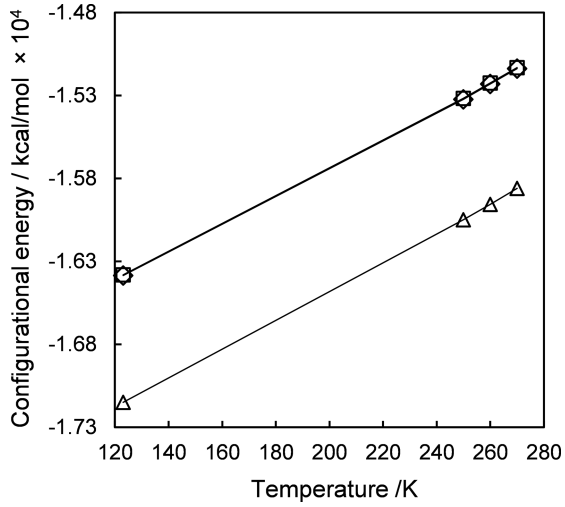

Figure 9. Change in configurational energy (kcal/mol) for the simulation cell as a function of the temperature from 123 to 270 K: the hypothetical PL sII hydrate (◊), the THF sII hydrate (□), and the PL + CH_4 sII clathrate hydrate (△).

interactions between PL and water not captured by classical molecular dynamics simulation, such as proton transfer from water to the basic PL molecule, can contribute to destabilizing the PL inclusion in pure PL hydrate. Furthermore, as well as THF, in solution phase, pyrrolidine changes the activity of water and reduces the melting point of hexahydrate and probably also clathrate hydrate.

4. CONCLUSION

In this study, we formed PL hydrates with the assistance of tetrahydrofuran (THF) which is a widely used large guest (LG) for sII hydrates. We characterized the pyrrolidine (PL) containing hydrates by melting temperature measurements, single-crystal X-ray diffraction, and solution-state NMR spectroscopy. With an increase of the PL ratio in the aqueous phase, the melting temperature decreased. The solution NMR measurements of melt solutions of the hydrate crystals clearly showed that PL was incorporated in the hydrate phase. Lattice constants which were determined by single-crystal X-ray

https://doi.org/10.1021/acs.cgd.0c01745
Cryst. Growth Des. 2021, 21, 2828−2836

diffraction increased with an increase of ϕ_{PL}. Inspection of the cage size found that $5^{12}6^4$ cages expand due to PL inclusion and that the empty 5^{12} cage slightly follows the $5^{12}6^4$ cage expansion. The refined structure of the crystal with $\phi_{PL} = 0.36$ ($\Phi = 0.502$) suggests that the PL is incorporated in the large cage without making hydrogen bonds stable to the cage water molecules. The MD simulations also support weak hydrogen bond interactions between PL and water molecules which may destabilize the structure of pure PL hydrate. The present results show that incorporation of PL requires expansion of the large cage of the sII clathrate hydrate, and distortion of the unit cell structure leads to the small cages needing support by small guests to become stable. This is also likely to be a structural stabilization mechanism for such LGs that need a *help gas* such as cyclohexane[67] and a key to further modification of the hydrate structure by introducing water-miscible LGs for improving the operating conditions of hydrate based technologies.

■ ASSOCIATED CONTENT

Supporting Information

The Supporting Information is available free of charge at https://pubs.acs.org/doi/10.1021/acs.cgd.0c01745.

Experimental and computational data (PDF)

Accession Codes

CCDC 2045524 contains the supplementary crystallographic data for this paper. These data can be obtained free of charge via www.ccdc.cam.ac.uk/data_request/cif, or by emailing data_request@ccdc.cam.ac.uk, or by contacting The Cambridge Crystallographic Data Centre, 12 Union Road, Cambridge CB2 1EZ, UK; fax: +44 1223 336033.

■ AUTHOR INFORMATION

Corresponding Author

Sanehiro Muromachi − *Energy Process Research Institute (EPRI), National Institute of Advanced Industrial Science and Technology (AIST), Tsukuba 305-8569, Japan; Department of Chemical and Biological Engineering, The University of British Columbia, Vancouver V6T 1Z3, Canada;* orcid.org/0000-0001-6121-4780; Phone: +81-29-861-4287; Email: s-muromachi@aist.go.jp; Fax: +81-29-861-8706

Authors

Hassan Sharifi − *Department of Chemical and Biological Engineering, The University of British Columbia, Vancouver V6T 1Z3, Canada*

Saman Alavi − *National Research Council of Canada, Ottawa, Ontario K1A 0R6, Canada;* orcid.org/0000-0001-9463-8766

John A. Ripmeester − *National Research Council of Canada, Ottawa, Ontario K1A 0R6, Canada;* orcid.org/0000-0002-4091-5120

Peter Englezos − *Department of Chemical and Biological Engineering, The University of British Columbia, Vancouver V6T 1Z3, Canada;* orcid.org/0000-0003-1569-4626

Complete contact information is available at: https://pubs.acs.org/10.1021/acs.cgd.0c01745

Author Contributions

S.M. performed all the experiments. S.A. performed the MD simulations. All authors contributed to the discussions and wrote the manuscript.

Notes

The authors declare no competing financial interest.

■ ACKNOWLEDGMENTS

S.M. acknowledges the Department of Energy and Environment in AIST for supporting fellowship program. P.E. acknowledges support from the Natural Sciences and Engineering Research Council of Canada.

■ REFERENCES

(1) Davidson, D. W. Clathrate Hydrates. In *Water A Comprehensive Treatise*; Franks, F., Ed.; Plenum Press: New York, 1973; pp 115−234, DOI: 10.1007/978-1-4757-6958-6_3.

(2) Jeffrey, G. A. Hydrate inclusion compounds. In *Inclusion Compounds*; Atwood, J. L., Davies, J. E., MacNicol, D. D., Eds.; Academic Press: New York, 1984; Vol. *1*.

(3) Sloan, E. D.; Koh, C. A. *Clathrate Hydrates of Natural Gases*, 3rd ed.; CRC Press: Boca Raton, FL, 2008; DOI: 10.1201/9781420008494.

(4) Seo, Y.; Kang, S. P.; Lee, S.; Lee, H. Experimental measurements of hydrate phase equilibria for carbon dioxide in the presence of THF, propylene oxide, and 1, 4-dioxane. *J. Chem. Eng. Data* **2008**, *53*, 2833−7.

(5) Lee, Y. J.; Kawamura, T.; Yamamoto, Y.; Yoon, J. H. Phase Equilibrium Studies of Tetrahydrofuran (THF) + CH_4, THF + CO_2, CH_4 + CO_2, and THF + CO_2 + CH_4 Hydrates. *J. Chem. Eng. Data* **2012**, *57*, 3543−3548.

(6) Veluswamy, H. P.; Kumar, A.; Seo, Y.; Lee, J. D.; Linga, P. A review of solidified natural gas (SNG) technology for gas storage via clathrate hydrates. *Appl. Energy* **2018**, *216*, 262−285.

(7) Sharifi, H.; Yoneyama, A.; Takeya, S.; Ripmeester, J.; Englezos, P. Superheating Clathrate Hydrates for Anomalous Preservation. *J. Phys. Chem. C* **2018**, *122*, 17019−17023.

(8) Babu, P.; Nambiar, A.; He, T.; Karimi, I. A.; Lee, J. D.; Englezos, P.; Linga, P. A Review of Clathrate Hydrate Based Desalination To Strengthen Energy−Water Nexus. *ACS Sustainable Chem. Eng.* **2018**, *6*, 8093−8107.

(9) Lee, J.; Kim, K. S.; Seo, Y. Thermodynamic, structural, and kinetic studies of cyclopentane + CO_2 hydrates: Applications for desalination and CO2 capture. *Chem. Eng. J.* **2019**, *375*, 121974.

(10) Babu, P.; Linga, P.; Kumar, R.; Englezos, P. A review of the hydrate based gas separation (HBGS) process for carbon dioxide pre-combustion capture. *Energy* **2015**, *85*, 261−279.

(11) International Energy Agency, *Energy Technology Perspectives*; 2017.

(12) International Energy Agency, *Technology roadmap − High-Efficiency, Low-Emissions Coal-Fired Power Generation*; 2012.

(13) Yang, H.; Xu, Z.; Fan, M.; Gupta, R.; Slimane, R. B.; Bland, A. E.; Wright, I. Progress in carbon dioxide separation and capture: A review. *J. Environ. Sci.* **2008**, *20*, 14−27.

(14) MacDowell, N.; Florin, N.; Buchard, A.; Hallett, J.; Galindo, A.; Jackson, G.; Adjiman, C. S.; Williams, C. K.; Shah, N.; Fennell, P. An overview of CO2 capture technologies. *Energy Environ. Sci.* **2010**, *3*, 1645−1669.

(15) D'Alessandro, D. M.; Smit, B.; Long, J. R. Carbon dioxide capture: Prospects for new materials. *Angew. Chem., Int. Ed.* **2010**, *49*, 6058−6082.

(16) Kang, S. P.; Lee, H.; Lee, C. S.; Sung, W. M. Hydrate phase equilibria of the guest mixtures containing CO_2, N_2 and tetrahydrofuran. *Fluid Phase Equilib.* **2001**, *185*, 101−109.

(17) Kumar, R.; Wu, H. J.; Englezos, P. Incipient hydrate phase equilibrium for gas mixture containing hydrogen, carbon dioxide and propane. *Fluid Phase Equilib.* **2006**, *244*, 167−171.

(18) Duc, N. H.; Chauvy, F.; Herri, J. M. CO_2 capture by hydrate crystallization - A potential solution for gas emission of steelmaking industry. *Energy Convers. Manage.* **2007**, *48*, 1313−1322.
(19) Kumar, R.; Englezos, P.; Moudrakovski, I.; Ripmeester, J. A. Structure and composition of CO_2/H_2 and $CO_2/H_2/C_3H_8$ hydrate in relation to simultaneous CO_2 capture and H_2 production. *AIChE J.* **2009**, *55*, 1584−1594.
(20) Kumar, R.; Lang, S.; Englezos, P.; Ripmeester, J. A. Application of the ATR-IR spec-troscopic technique to the characterization of hydrates formed by CO2, CO2/H2 and CO2 /H2 /C3H 8. *J. Phys. Chem. A* **2009**, *113*, 6308−6313.
(21) Lee, Y.; Lee, S.; Lee, J.; Seo, Y. Structure identification and dissociation enthalpy measurements of the CO_2 + N_2 hydrates for their application to CO_2 capture and storage. *Chem. Eng. J.* **2014**, *246*, 20−26.
(22) Babu, P.; Linga, P.; Kumar, R.; Englezos, P. A review of the hydrate based gas separation (HBGS) process for carbon dioxide pre-combustion capture. *Energy* **2015**, *85*, 261−279.
(23) Ma, Z. W.; Zhang, P.; Bao, H. S.; Deng, S. Review of fundamental properties of CO_2 hydrates and CO_2 capture and separation using hydration method. *Renewable Sustainable Energy Rev.* **2016**, *53*, 1273−302.
(24) Narayanan, T. M.; Ohmura, R. Influence of hydrate structure on continuous separation of coal bed methane gas: A thermodynamic simulation study. *J. Nat. Gas Sci. Eng.* **2016**, *35*, 1511−1518.
(25) Kim, S.; Choi, S.-D.; Seo, Y. CO2 capture from flue gas using clathrate formation in the presence of thermodynamic promoters. *Energy* **2017**, *118*, 950−956.
(26) Horii, S.; Ohmura, R. Continuous separation of CO_2 from a H_2 + CO_2 gas mixture using clathrate hydrate. *Appl. Energy* **2018**, *225*, 78−84.
(27) Mooijer-van den Heuvel, M. M.; Witteman, R.; Peters, C. J. Phase behaviour of gas hydrates of carbon dioxide in the presence of tetrahydropyran, cyclobutanone, cyclohexane and methylcyclohexane. *Fluid Phase Equilib.* **2001**, *182*, 97−110.
(28) Iino, K.; Takeya, S.; Ohmura, R. Characterization of clathrate hydrates formed with CH_4 or CO_2 plus tetrahydropyran. *Fuel* **2014**, *122*, 270−276.
(29) Susilo, R.; Ripmeester, J. A.; Englezos, P. Characterization of gas hydrates with PXRD, DSC, NMR, and Raman spectroscopy. *Chem. Eng. Sci.* **2007**, *62*, 3930−3939.
(30) Poling, B. E.; Prausnitz, J. M.; O'Connell, J. P. *Properties of Gases and Liquids*, 5th ed.; McGraw-Hill Education: New York, 2000.
(31) Rochelle, G. T. Amine scrubbing for CO_2 capture. *Science* **2009**, *325*, 1652−1654.
(32) Shin, W.; Park, S.; Ro, H.; Koh, D. Y.; Seol, J.; Lee, H. Phase equilibrium measurements and the tuning behavior of new sII clathrate hydrates. *J. Chem. Thermodyn.* **2012**, *44*, 20−25.
(33) Lee, S.; Lee, Y.; Park, S.; Kim, Y.; Lee, J. D.; Seo, Y. Structural Transformation of Isopropylamine Semiclathrate Hydrates in the Presence of Methane as a Coguest. *J. Phys. Chem. B* **2012**, *116*, 9075−9081.
(34) Cha, M.; Lee, H.; Lee, J. W. Thermodynamic and Spectroscopic Identification of Methane Inclusion in the Binary Heterocyclic Compound Hydrates. *J. Phys. Chem. C* **2013**, *117*, 23515−23521.
(35) Park, S.; Kang, H.; Shin, K.; Seo, Y.; Lee, H. Structural transformation and tuning behavior induced by the propylamine concentration in hydrogen clathrate hydrates. *Phys. Chem. Chem. Phys.* **2015**, *17*, 1949−1956.
(36) Dobrzycki, L.; Taraszewska, P.; Boese, R.; Cyranski, M. K. Pyrrolidine and Its Hydrates in the Solid State. *Cryst. Growth Des.* **2015**, *15*, 4804−4812.
(37) Imasato, K.; Murayama, K.; Takeya, S.; Alavi, S.; Ohmura, R. Effect of nitrogen atom substitution in cyclic guests on properties of structure H clathrate hydrates. *Can. J. Chem.* **2015**, *93*, 906−912.
(38) Dobrzycki, L.; Socha, P.; Ciesielski, A.; Boese, R.; Cyranski, M. K. Formation of Crystalline Hydrates by Nonionic Chaotropes and Kosmotropes: Case of Piperidine. *Cryst. Growth Des.* **2019**, *19*, 1005−1020.
(39) Carbonnel, L.; Rosso, J. C.; Caranoni, C. New variety of heterocycles generating cubic clathrate hydrates - binary-system water-pyrrolidine. *C. R. Seances Acad. Sci., Ser. C* **1973**, *276* (8), 619−622.
(40) Desmedt, A.; Martin-Gondre, L.; Nguyen, T. T.; Petuya, C.; Barandiaran, L.; Babot, O.; Toupance, T.; Grim, G. R.; Sum, A. K. Modifying the Flexibility of Water Cages by Co-Including Acidic Species within Clathrate Hydrate. *J. Phys. Chem. C* **2015**, *119*, 8904−8911.
(41) Shin, K.; Moudrakovski, I. L.; Davari, M. D.; Alavi, S.; Ratcliffe, C. I.; Ripmeester, J. A. Crystal engineering the clathrate hydrate lattice with NH_4F. *CrystEngComm* **2014**, *16*, 7209−7219.
(42) Takeya, S.; Alavi, S.; Hashimoto, S.; Yasuda, K.; Yamauchi, Y.; Ohmura, R. Distortion of the Large Cages Encapsulating Cyclic Molecules and Empty Small Cages of Structure II Clathrate Hydrates. *J. Phys. Chem. C* **2018**, *122*, 18134−18141.
(43) Sheldrick, G. M. Phase Annealing in SHELX-90: Direct Methods for Larger Structures. *Acta Crystallogr., Sect. A: Found. Crystallogr.* **1990**, *46*, 467−473.
(44) Todorov, I. T.; Smith, W.; Trachenko, K.; Dove, M. T. *J. Mater. Chem.* **2006**, *16*, 1911−1918.
(45) Takeuchi, F.; Hiratsuka, M.; Ohmura, R.; Alavi, S.; Sum, A. K.; Yasuoka, K. Water Proton Configurations in Structures I, II, and H Clathrate Hydrate Unit Cells. *J. Chem. Phys.* **2013**, *138*, 124504.
(46) Abascal, J. L. F.; Vega, C. A general purpose model for the condensed phases of water: TIP4P/2005. *J. Chem. Phys.* **2005**, *123*, 234505.
(47) Cornell, W. D.; Cieplak, P.; Bayly, C. L.; Gould, I. R.; Merz, K. M.; Ferguson, D. M.; Spellmeyer, D. C.; Fox, T.; Caldwell, J. W.; Kollman, P. A. A Second Generation Force Field for the Simulation of Proteins, Nucleic Acid, and Organic Molecules. *J. Am. Chem. Soc.* **1995**, *117*, 5179−5197.
(48) Wang, J.; Wolf, R. M.; Caldwell, J. W.; Kollman, P. A.; Case, D. A. Development and testing of a general AMBER force field. *J. Comput. Chem.* **2004**, *25*, 1157−1174.
(49) Eggimann, B. L.; Sunnarborg, A. J.; Stern, H. D.; Bliss, A. P.; Siepmann, J. I. An online parameter and property database for the TraPPE force field. Mol. Sim. *Mol. Simul.* **2014**, *40*, 101−105.
(50) Breneman, C. M.; Wiberg, K. B. Determining atom-centered monopoles from molecular electrostatic potentials. The need for high sampling density in formamide conformational analysis. *J. Comput. Chem.* **1990**, *11*, 361−373.
(51) Frisch, M. J.; Trucks, G. W.; Schlegel, H. B.; Scuseria, G. E.; Robb, M. A.; Cheeseman, J. R.; Scalmani, G.; Barone, V.; Mennucci, B.; Petersson, G. A.; Nakatsuji, H.; Caricato, M.; Li, X.; Hratchian, H. P.; Izmaylov, A. F.; Bloino, J.; Zheng, G.; Sonnenberg, J. L.; Hada, M.; Ehara, M.; Toyota, K.; Fukuda, R.; Hasegawa, J.; Ishida, M.; Nakajima, T.; Honda, Y.; Kitao, O.; Nakai, H.; Vreven, T.; Montgomery, J. A., Jr.; Peralta, J. E.; Ogliaro, F.; Bearpark, M.; Heyd, J. J.; Brothers, E.; Kudin, K. N.; Staroverov, V. N.; Kobayashi, R.; Normand, J.; Raghavachari, K.; Rendell, A.; Burant, J. C.; Iyengar, S. S.; Tomasi, J.; Cossi, M.; Rega, N.; Millam, J. M.; Klene, M.; Knox, J. E.; Cross, J. B.; Bakken, V.; Adamo, C.; Jaramillo, J.; Gomperts, R.; Stratmann, R. E.; Yazyev, O.; Austin, A. J.; Cammi, R.; Pomelli, C.; Ochterski, J. W.; Martin, R. L.; Morokuma, K.; Zakrzewski, V. G.; Voth, G. A.; Salvador, P.; Dannenberg, J. J.; Dapprich, S.; Daniels, A. D.; Farkas, Ö.; Foresman, J. B.; Ortiz, J. V.; Cioslowski, J.; Fox, D. J. *Gaussian 09, Revision E.01*; Gaussian, Inc.: Wallingford, CT, 2009.
(52) Pfafferott, G.; Oberhammer, H.; Boggs, J. E.; Caminati, W. Geometric structure and psuedorotation of pyrrolidine. An ab initio and electron diffraction stude. *J. Am. Chem. Soc.* **1985**, *107*, 2305−2309.
(53) Carballeira, L.; Pérez-Juste, I.; Van Alsenoy, C. Theoretical study of pyrrolidine: Revised conformational energies and vibrational assignments. *J. Phys. Chem. A* **2002**, *106*, 3873−3884.
(54) Kunitski, M.; Riehn, C.; Matylitsky, V. V.; Tarakeshwar, P.; Brutschy, B. Pseudorotation in pyrrolidine: rotational coherence

https://doi.org/10.1021/acs.cgd.0c01745
Cryst. Growth Des. 2021, 21, 2828−2836

spectroscopy and ab initio calculations of a large amplitude intramolecular motion. *Phys. Chem. Chem. Phys.* **2010**, *12*, 72−81.
(55) Hesse, S.; Wassermann, T. N.; Suhm, M. A. Brightening and locking a weak and floppy N- H chromophore: The case of pyrrolidine. *J. Phys. Chem. A* **2010**, *114*, 10492−10499.
(56) Dziubek, K. F.; Katrusiak, A. Pressure-induced pseudorotation in crystalline pyrrolidine. *Phys. Chem. Chem. Phys.* **2011**, *13*, 15428−15431.
(57) Allen, M. P.; Tildesley, D. J. *Computer Simulation of Liquids*; Oxford Science Publications: Oxford, 1987; DOI: 10.1093/oso/9780198803195.001.0001.
(58) Frenkel, D.; Smit, B. *Understanding Molecular Simulation*; Academic Press: San Diego, 2000; DOI: 10.1016/B978-0-12-267351-1.X5000-7.
(59) Otake, K.; Tsuji, T.; Sato, I.; Akiya, T.; Sako, T.; Hongo, M. A proposal of a new technique for the density measurements of solids. *Fluid Phase Equilib.* **2000**, *171*, 175−179.
(60) Anderson, R.; Chapoy, A.; Tohidi, B. Phase relations and binary clathrate hydrate formation in the system H_2−THF−H_2O. *Langmuir* **2007**, *23*, 3440−3444.
(61) Makino, T.; Sugahara, T.; Ohgaki, K. Stability boundaries of tetrahydrofuran + water system. *J. Chem. Eng. Data* **2005**, *50*, 2058−2060.
(62) Delahaye, A.; Fournaison, L.; Marinhas, S.; Chatti, I.; Petitet, J. P.; Dalmazzone, D.; Furst, W. Effect of THF on Equilibrium Pressure and Dissociation Enthalpy of CO_2 Hydrates Applied to Secondary Refrigeration. *Ind. Eng. Chem. Res.* **2006**, *45*, 391−397.
(63) Schlenk, W. Die thioharnstoff-addition organischer verbindungen. *Annalen Der Chemie-Justus Liebig* **1951**, *573* (2), 142−162.
(64) Shin, K.; Udachin, K. A.; Moudrakovski, I. L.; Leek, D. M.; Alavi, S.; Ratcliffe, C. I.; Ripmeester, J. A. Methanol incorporation in clathrate hydrates and the implications for oil and gas pipeline flow assurance and icy planetary bodies. *Proc. Natl. Acad. Sci. U. S. A.* **2013**, *110*, 8437−8442.
(65) Tse, J. S. Thermal-expansion of the clathrate hydrates of ethylene-oxide and tetrahydrofuran. *Journal De Physique* **1987**, *48* (C-1), C1-543−C1-549.
(66) Udachin, K. A.; Ratcliffe, C. I.; Ripmeester, J. A. Single Crystal Diffraction Studies of Structure I, II and H Hydrates: Structure, Cage Occupancy and Composition. *J. Supramol. Chem.* **2002**, *2*, 405−408.
(67) Tohidi, B.; Danesh, A.; Burgass, R. W.; Todd, A. C. Equilibrium Data and Thermodynamic Modelling of Cyclohexane Gas Hydrates. *Chem. Eng. Sci.* **1996**, *51* (1), 159−163.

https://doi.org/10.1021/acs.cgd.0c01745
Cryst. Growth Des. 2021, 21, 2828−2836